VIII International Conference on Computational Methods for Coupled Problems in Science and Engineering
COUPLED PROBLEMS 2019
E. Oñate, M. Papadrakakis and B. Schrefler (Eds)

NUMERICAL AND ANALYTICAL INVESTIGATION OF SUBCYCLING IN THE FLOW PROBLEM OF A STRONGLY-COUPLED PARTITIONED FLUID-STRUCTURE INTERACTION SIMULATION

LAURENT DE MOERLOOSE* AND JORIS DEGROOTE†

*Department of Flow, Heat and Combustion Mechanics, Ghent University
Sint-Pietersnieuwstraat 41-B4, 9000 Ghent, Belgium
e-mail: laurent.demoerloose@ugent.be

†Department of Flow, Heat and Combustion Mechanics, Ghent University
Sint-Pietersnieuwstraat 41-B4, 9000 Ghent, Belgium
Flanders Make, Belgium
e-mail: joris.degroote@ugent.be

Key words: Subcycling, temporal stability, fluid-structure interaction

Abstract. Fluid-structure interaction (FSI) simulations can be used to quantify the frequency, damping constant and amplitude of the vibration of equipment such as piping and heat exchangers. Typically, the time step is the same in the flow and structural equations, but this causes long computational times when the time step is restricted due to stability requirements of only one solver. In that case, a more efficient approach is to use so-called subcycling with a different time step in the flow and structural solver. In this paper, only subcycling with a smaller time step in the flow solver compared to the structural solver is analyzed. The research presented here is split into two parts: an analytical study and a numerical computation of the one-dimensional flow in an elastic cylindrical tube. Firstly, a monolithic analytical FSI calculation is analyzed with a Fourier stability analysis. This allows to verify the stability of the solution by considering the eigenvalues of the problem as a function of the perturbation wavenumber. The conclusions drawn from the analytical study are subsequently verified in a partitioned numerical FSI simulation, coupling the flow solver Fluent with the structural solver Abaqus. The implicit coupling is achieved using an interface quasi-Newton method with an approximation of the inverse of the Jacobian (IQN-ILS), implemented in the in-house code Tango. The research shows that a stable solution is attained for significant subcycling in the flow problem: the results indicate that the solution remains temporally stable even if the time step in the flow solver is only one tenth of the structural time step. However, some (temporally stable) oscillations in the resulting pressure profile on the pipe wall arise when the time discretization schemes applied in the flow and structural solvers are different. These oscillations do not persist when the same time discretization scheme is applied.

1 INTRODUCTION

With the available modern-day computing power, fluid-structure interaction (FSI) simulations are becoming increasingly interesting for the study of movement-induced vibrations, in which a flow causes the motion or deformation of a structure. FSI is also used to determine the fluid-elastic properties of structural vibrations with more limited amplitude, such as to avoid fretting in tube arrays subjected to axial flow [1].

In most FSI cases, the flow and structural solver apply the same time step in transient simulations, even though the maximal time step required for stability or accuracy reasons in the flow solver is in most cases significantly smaller than in the structural solver. Since a coupling iteration happens at least once during every timestep, the required CPU time is large even though the structure barely moves during one time step. A more efficient algorithm requires the definition of a smaller time step for the flow solver and a larger time step for the structural solver. Accordingly, multiple (smaller) time steps are performed in the flow solver before performing a coupling iteration and performing one (larger) time step in the structural solver. This procedure is called subcycling.

Most previous work [2, 3] perform stability analyses on explicit subcycling. In that case, no coupling iterations occur between the flow and structural solver within a single time step. We consider a flow solver and a structural solver, respectively with time steps Δt_F and Δt_S, such that a number $N_{S/F}$ is defined as: $N_{S/F} = \Delta t_S / \Delta t_F$. In this paper, $N_{S/F}$ is defined as a positive integer. The difficulty is to determine how the total fluid-structure interface displacement in a time step Δt_S should be interpolated in the $N_{S/F}$ subcycles in the flow solver. Additionally, the question is what interface load should be transmitted to the structural solver at the end of the $N_{S/F}$ subcycles. In the conventional explicit subcycling procedure [3], the interface pressure at the end of the last subcycling step is transmitted to the structure. The disadvantage of this approach is that the time step required to achieve a stable solution is limited and possibly lower than the time step limit imposed by the flow solver itself. In contrast, the stability of the explicit subcycling method is preserved when two conditions are met. Firstly, the predicted displacement over one time step Δt_S is evenly distributed among the $N_{S/F}$ subcycles. Secondly, the average interface pressure field computed during the $N_{S/F}$ subcycles is fed to the structural solver.

Contrary to explicit subcycling, little research can be found about implicit subcycling. Probably, this is due to the fact that explicit subcycling is inherently easier to define as all flow and structure variables are only calculated once. As such, explicit coupling is more flexible with respect to the use of different time steps in the solvers [4]. On the other hand, it is well-established that there are FSI problems for which the explicit coupling does not reach convergence, e.g. in high density fluids [5]. In those cases, implicit coupling is required to reach a stable solution, which is why more research into implicit subcycling is needed [6].

In this paper, the temporal stability of an implicit coupling scheme with subcycling in the flow solver is investigated. Firstly, a monolithic analytical study on a one-dimensional

model for flow in an elastic tube is presented. Secondly, a numerical partitioned strongly-coupled FSI simulation is reported. Both methods are described in Section 2. The results of both methods are subsequently compared in Section 3.

2 METHOD

2.1 Analytical monolithic FSI calculation

In order to investigate the temporal stability of the subcycling in the flow solver, the eigenvalues of the matrix relating the variables in consecutive time steps are calculated. A monolithic approach is therefore more straightforward in the analytical study than a partitioned approach, but the result of the study would be the same for a partitioned scheme (as only the temporal stability of the problem is discussed, not the stability of the coupling iterations between flow and structural solver). The fluid-structure interface condition is of the Dirichlet-Neumann type: the displacement of the structure is used as a boundary condition for the flow equations while the fluid pressure is imposed in the structural equations.

2.1.1 Governing equations

The test case is comprised of a one-dimensional flow in a straight, flexible tube shown schematically in Figure 1. The equations that describe the unsteady flow of the incompressible fluid are the continuity and the momentum equation, given by

$$\frac{\partial s}{\partial t} + \frac{\partial su}{\partial x} = 0 \tag{1a}$$

$$\frac{\partial su}{\partial t} + \frac{\partial su^2}{\partial x} + \frac{1}{\rho_f}\left(\frac{\partial s\hat{p}}{\partial x} - \hat{p}\frac{\partial s}{\partial x}\right) = 0 \tag{1b}$$

in which s represents the cross sectional area of the tube, u the axial velocity, x the axial coordinate, t the time, ρ_f the fluid density and $\hat{p}$ the pressure. In the remainder of this paper, the kinematic pressure $p = \hat{p}/\rho_f$ will be used. It is noted that gravity and viscous terms are not considered. In the structural subproblem, the radial deformation of the elastic tube is modelled by

$$\rho_s h\frac{\partial^2 r}{\partial t^2} + \chi\frac{\partial^4 r}{\partial x^4} - \psi\frac{\partial^2 r}{\partial x^2} + \eta(r - r_0) = \rho_f(p - p_0) \tag{1c}$$

with r describing the inner radius, ρ_s the wall density, h the wall thickness and p_0 the pressure corresponding to the reference radius at rest r_0. Considering the negligence of gravity and viscous terms in the flow equations, the tube deformation in other dimensions (both longitudinal and circumferential) is not considered. As such, the proposed structural model is an extension to the so-called independent-rings model [7], as the terms containing χ and ψ take into account the longitudinal interaction between the tube segments. ψ is equivalent to $\kappa G h$ with κ the Timoshenko shear correction factor and G the shear modulus. η is given by $Eh/(1-\nu^2)r_0^2$ with E the Young's modulus and ν the Poisson's ratio.

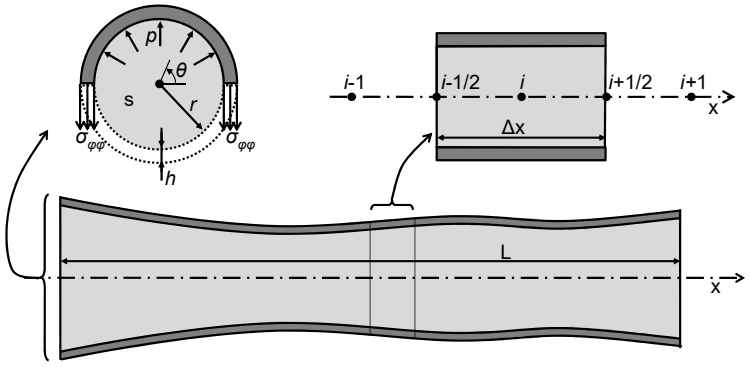

Figure 1: Schematic of the one-dimensional flow through a straight, elastic tube.

2.1.2 Spatial discretization

The tube with length L is discretized in N spatial intervals of equal length Δx. Central discretization is used for all terms appearing in the flow and structural equations, except for the convective term in the momentum equation. For the latter, a first-order upwind scheme is applied. In the following equations, subscripts i and $i \pm 1/2$ indicate cell centers and faces, respectively.

To allow for analytic manipulation, the velocity, radius and pressure are expressed as the sum of a reference value (indicated with a subscript 0) and a perturbation term (indicated with a prime). Artificial diffusion is added in the continuity equation with coefficient [8]: $\delta = s_0/\pi/(u_0 + \Delta x/\Delta t)$. This term is used to stabilize the pressure equation and disappears upon convergence of the solution. After linearization of the equations, the following is obtained:

$$\Delta x \frac{\partial 2 r_0 r_i^{'}}{\partial t} + {r_0}^2 (u_{i+1/2}^{'} - u_{i-1/2}^{'}) + 2 r_0 u_0 (r_{i+1/2}^{'} - r_{i-1/2}^{'}) - \delta (p_{i+1}^{'} - 2 p_i^{'} + p_{i-1}^{'}) = 0 \quad (2a)$$

$$\Delta x \frac{\partial \left(r_0^2 u_i^{'} + 2 r_0 u_0 r_i^{'} \right)}{\partial t} + {r_0}^2 u_0 (u_i^{'} - u_{i-1}^{'} + u_{i+1/2}^{'} - u_{i-1/2}^{'} + 2 r_0 u_0^2 (r_{i+1/2}^{'} - r_{i-1/2}^{'}) + \frac{1}{2} r_0^2 (p_{i+1}^{'} - p_{i-1}^{'}) = 0 \quad (2b)$$

$$\rho_s h \frac{\partial^2 r_i^{'}}{\partial t^2} + \frac{\chi}{\Delta x^4} (r_{i+2}^{'} - 4 r_{i+1}^{'} + 6 r_i^{'} - 4 r_{i-1}^{'} + r_{i-2}^{'}) - \frac{\psi}{\Delta x^2} (r_{i+1}^{'} - 2 r_i^{'} + r_{i-1}^{'}) + \eta \left(r_i^{'} \right) = \rho_f \left(p_i^{'} \right) \quad (2c)$$

for $u_i \geq 0$. Subsequently, the pressure, radius and velocity perturbation are then decomposed as the sum of N Fourier modes (in the spatial dimension). For example, the radius

perturbation is defined as:

$$r_i^{'} = \frac{1}{N}\sum_{l=0}^{N-1} \tilde{r}_l \exp(\jmath\omega_l i\Delta x) \tag{3}$$

with $\omega_l = 2\pi l/L$ the wave number. Equation (3) is substituted into Equation (2). A similar procedure is applied to the velocity and pressure perturbation. Afterwards, Equation (2) is projected on $\exp(\jmath\omega_\ell i\Delta x)$, which allows to investigate the temporal stability of each wave component independently. The latter is possible due to the linear nature of Equation (2). In the following equations, the product $\omega_\ell\Delta x$ is substituted by θ_ℓ. The tilde and subscripts are omitted.

$$\Delta x\frac{\partial 2r_0 r}{\partial t} + \jmath r_0^2\sin(\theta)u + 2\jmath r_0 u_0\sin(\theta)r + 2\delta(1-\cos(\theta))p = 0 \tag{4a}$$

$$\Delta x\frac{\partial\left(r_0^2 u + 2r_0u_0 r\right)}{\partial t} + (1-\exp(-\jmath\theta)+\jmath\sin(\theta))r_0^2u_0u + 2\jmath u_0^2 r_0\sin(\theta)r + \jmath r_0^2\sin(\theta)p = 0 \tag{4b}$$

$$\rho_s h\frac{\partial^2 r}{\partial t^2} + \left(\frac{4\chi}{\Delta x^4}(1-\cos(\theta))^2 + \frac{2\psi}{\Delta x^2}(1-\cos(\theta)) + \eta\right) r = \rho_f p \tag{4c}$$

2.1.3 Temporal discretization

The backward Euler scheme (BE) is used for the time discretization of the flow equations. Using higher-order schemes would lead to the presence of multiple older time steps in the equations, which was not desirable in the current analytical study. The BE scheme results in the following equation:

$$\frac{2r_0\Delta x}{\Delta t_f}(r^{n+1}-r^n) + \jmath r_0^2\sin(\theta)u^{n+1} + 2\jmath r_0u_0\sin(\theta)r^{n+1} + 2\delta(1-\cos(\theta))p^{n+1} = 0 \tag{5a}$$

$$\frac{r_0^2\Delta x}{\Delta t_f}(u^{n+1}-u^n) + \frac{2r_0u_0\Delta x}{\Delta t_f}(r^{n+1}-r^n) + (1-\exp(-\jmath\theta)+\jmath\sin(\theta))r_0^2u_0u^{n+1} + 2\jmath u_0^2r_0\sin(\theta)r^{n+1} + \jmath r_0^2\sin(\theta)p^{n+1} = 0 \tag{5b}$$

For the temporal discretization of the structure, a logical choice is the use of the BE scheme in order to have the same time discretization in the flow and structural solver. However, the scheme defined by Hilber, Hughes and Taylor (HHT) [9] is more common for structures. Therefore, both discretization schemes will be discussed. The BE scheme for the structure yields:

$$\rho_s h\ddot{r}^{n+1} + \left(\frac{4\chi}{\Delta x^4}(1-\cos(\theta))^2 + \frac{2\psi}{\Delta x^2}(1-\cos(\theta)) + \eta\right) r^{n+1} = \rho_f p^{n+1} \tag{6a}$$

in which the acceleration and velocity are calculated as

$$\ddot{r}^{n+1} = \frac{1}{\Delta t_s}(\dot{r}^{n+1} - \dot{r}^n) \qquad \text{and} \qquad \dot{r}^{n+1} = \frac{1}{\Delta t_s}(r^{n+1} - r^n). \tag{6b}$$

For the HHT scheme, the forces in Equation (4c) are defined as a weighted average of the forces at the beginning and end of the time step, with the variable α as weighting function. This discretization scheme is also imposed in the structural solver in the partitioned FSI simulation discussed in Section 2.2.

$$\begin{aligned}\rho_s h \ddot{r}^{n+1} + (1+\alpha)\left[\left(\frac{4\chi}{\Delta x^4}(1-\cos(\theta))^2 + \frac{2\psi}{\Delta x^2}(1-\cos(\theta)) + \eta\right) r^{n+1} - \rho_f p^{n+1}\right] \\ - \alpha\left[\left(\frac{4\chi}{\Delta x^4}(1-\cos(\theta))^2 + \frac{2\psi}{\Delta x^2}(1-\cos(\theta)) + \eta\right) r^{n} - \rho_f p^{n}\right] = 0\end{aligned} \tag{7a}$$

The operator definition is completed by the Newmark formula [10] for acceleration and velocity integration:

$$\ddot{r}^{n+1} = \frac{1}{\beta \Delta t_s^2}(r^{n+1} - r^n) - \frac{1}{\beta \Delta t_s}\dot{r}^n - \left(\frac{1}{2\beta} - 1\right)\ddot{r}^n \tag{7b}$$

$$\dot{r}^{n+1} = \dot{r}^n + \Delta t_s(1-\gamma)\ddot{r}^n + \Delta t_s \gamma \ddot{r}^{n+1} \tag{7c}$$

with $\alpha \in [-1/3, 0]$ determining the numerical dissipation, $\beta = (1-\alpha)^2/4$ and $\gamma = 1/2 - \alpha$.

2.2 Numerical partitioned FSI simulation

In order to verify the analytical results with a numerical simulation, a black-box flow solver is coupled to a black-box structural solver. As such, the FSI simulation is partitioned.

The flow equations are solved in an Arbitrary Lagrangian-Eulerian (ALE) formulation with the commercial code Fluent® 12.1, Ansys Inc. The fluid grid contains 10^4 cells and its deformation is computed from the solution of a system of linear springs located in between connected nodes of the mesh. The initial (undeformed) mesh is a structural mesh inside a rectangular domain. A first-order upwind scheme is used for the modelling of the convective terms. The BE scheme is selected for the temporal discretization of the flow equations. The parameters listed in Table 1 are used as numerical values for the flow in a tube. The fluid is considered incompressible and has a constant viscosity of 3 mPas. At the inlet, an axial fluid velocity of $u_0 + \frac{u_0}{2} sin(2\pi t) H(t)$ is imposed, where H represents the Heaviside function. Given an initial velocity field of $u_0 = 0.1\,\mathrm{m/s}$, the inlet velocity has a discontinuity in its derivative at $t = 0\,\mathrm{s}$. At this time, spurious modes can enter the solution. The temporal stability can be evaluated in the subsequent time steps. The pressure at the tube's outlet is set to the atmospheric pressure.

The structural equations are solved in a Lagrangian frame with the commercial finite-element solver Abaqus® 6.7, Dassault Systèmes. Both the BE and HHT scheme are

applied to the structure equations. A structured grid of 2500 quadratic elements is constructed in the structural domain. Only radial deformation is allowed, similar to the analytical case described in Section 2.1.

The coupling between both solvers at the interface is done through a Dirichlet-Neumann boundary condition. As such, the flow solver computes the pressure and shear stress for a given mesh displacement. These output variables are subsequently transferred to the structural solver, which calculates the new deformation of the fluid-structure interface. The equilibrium at the fluid-structure interface is established using an interface quasi-Newton algorithm with an approximation for the inverse of the Jacobian from a least-squares model (IQN-ILS) [11]. The difference with the classical IQN-ILS algorithm is that more than 1 timestep is calculated in the flow solver before the structural solver is called. In a more mathematical description, the wrapper around the flow solver receives the data for t^{n+1} from the coupling code and gives the flow solver the command to perform $N_{S/F}$ time steps, while providing boundary displacements that are interpolated in time for each of those intermediate time steps. At the beginning of the next coupling iteration, the file from time step t^n is read in from the storage. A time step size Δt_s of 10^{-4} s is used.

For the coupling iterations, the convergence criterion in the Euclidean norm for the residual of the interface displacement is set to 10^{-8} m and for the residual of the interface load to 10^{-2} Pa. More severe convergence criteria have no significant impact on the results. Accordingly, the coupling iterations have completely converged. Therefore, this paper does not discuss the stability of the coupling iterations. Rather, this test case is used to determine whether the subcycling procedure is temporally stable or not. Since a monolithic solver with the same convergence criteria would yield the same solution as the applied partitioned solver in the numerical simulation, the numerical and analytical results discussed in Section 3 are directly comparable.

3 RESULTS

3.1 Analytical monolithic FSI calculation

In Equations (5-7), the same time step size was used for the time integration of the flow and the structure. For the analytic study of subcycling in the flow problem, the flow time step Δt_f is chosen equal to half of the structural time step Δt_s or, equivalently, $N_{S/F} = 2$. Hence, the variable $\Delta t_s = \Delta t$ is called 'a time step' and $\Delta t_f = \Delta t/2$ is referred to as 'a subcycle'.

An important aspect of subcycling is to determine the appropriate interpolation of the displacement of the fluid-structure interface during consecutive subcycles. In order to obtain a continuous acceleration in each node of the interface - which is desirable to obtain a numerically stable solution - a third degree polynomial per point on the interface is used to prescribe the wall displacement during time step $n + 1$. The four parameters in this polynomial are: the wall displacements at the beginning and the end of the time step (r^n and r^{n+1}) and the wall accelerations at the beginning and the end of the time

Table 1: Dimensions of the model and material properties.

E	300000	$\mathrm{N/m^2}$	ν	0.49	
χ	0	$\mathrm{kg\,m^2/s^2}$	ψ	55	$\mathrm{kg/s^2}$
ρ_s	1200	$\mathrm{kg/m^3}$	ρ_f	1000	$\mathrm{kg/m^3}$
u_0	0.1	m/s	r_0	0.005	m
L	0.05	m	h	0.001	m

step ($\ddot{r}^n$ and $\ddot{r}^{n+1}$) as calculated by the structural solver. The wall displacement imposed during the first subcycle is then given by $r^{n+1/2} = \frac{r^{n+1}}{2} + \frac{r^n}{2} - \frac{3\ddot{r}^{n+1}\Delta t^2}{16} + \frac{\ddot{r}^n\Delta t^2}{16}$ and r^{n+1} during the second subcycle.

Two new variables are introduced: $u^{n+1/2}$ and $p^{n+1/2}$, representing the fluid velocity and the pressure at the intermediate time $n+1/2$ between time step n and $n+1$.

In case the BE scheme is used in both solvers, Equation (5) for the flow is changed to a corresponding system of equations at times $t^{n+1/2}$ and t^{n+1}, respectively. The structure problem is completely described with Equation (6). Next, these equations are transformed to the following matrix form:

$$Ay = Bz \tag{8a}$$

$$\text{with} \quad y = [r^{n+1}\ \dot{r}^{n+1}\ \ddot{r}^{n+1}\ r^{n+1/2}\ u^{n+1/2}\ u^{n+1}\ p^{n+1/2}\ p^{n+1}]^T \tag{8b}$$

$$\text{and} \quad z = [r^{n}\ \dot{r}^{n}\ \ddot{r}^{n}\ r^{n-1/2}\ u^{n-1/2}\ u^{n}\ p^{n-1/2}\ p^{n}]^T \tag{8c}$$

The variables $r^{n-1/2}$, $u^{n-1/2}$ and $p^{n-1/2}$ do not occur in any equation, but are added to obtain a square amplification matrix $A^{-1}B$. In case the BE scheme and the HHT scheme are used in the flow and the structural solver, respectively, the structure is instead governed by Equation (7). The flow equations do not change. For a more detailed description of the matrices A and B, the reader is referred to the work of De Moerloose et al. [6].

The parameters shown in Table 1 are used to calculate the eigenvalues of the amplification matrix $A^{-1}B$. The grid size is set to $\Delta x = 10^{-4}\,\mathrm{m}$ and the time step is chosen equal to $\Delta t = 10^{-5}\,\mathrm{s}$. The variable α is set to -0.07. For both combinations of time integration schemes, two eigenvalues of the amplification matrix $A^{-1}B$ are equal to one. Their eigenvectors correspond to the solution of the one-dimensional case. Additionally, three eigenvalues equal zero because the matrix B contains three zero-columns, corresponding to the variables $r^{n-1/2}$, $u^{n-1/2}$ and $p^{n-1/2}$ which do not occur in any equation. The stability of the FSI problem is thus determined by the absolute value of the remaining three eigenvalues.

3.1.1 BE-BE combination

As the variable p^n does not occur in the equations in the BE-BE combination, another eigenvalue is equal to zero, bringing the total to four (due to the absence of the variables

$r^{n-1/2}$, $u^{n-1/2}$, $p^{n-1/2}$ and p^n). The amplitude of the two remaining eigenvalues is shown in Figure 2a as a function of the wave number ω. Furthermore, performing a similar analysis on the system of Equations (5-6) without subcycling, yields only one relevant eigenvalue - the other eigenvalues are either equal to zero or one. This eigenvalue determines the temporal stability of the system without subcycling and is therefore also shown in Figure 2a. Even though the amplitude of the eigenvalues comes closer to one when subcycling is used, it remains smaller than one for all wavenumbers. It can be concluded that a stable solution should be obtained.

3.1.2 BE-HHT combination

In case the HHT operator is used for the structure combined with the BE scheme for the flow, only three eigenvalues are equal to zero. The amplitude of the three remaining eigenvalues is shown in Figure 2b. Contrary to what was observed in Section 3.1.1, the use of subcycling reduces the amplitude of the eigenvalues of the BE-HHT scheme (compared to the calculation without subcycling). Therefore, the FSI problem also remains stable for all wave numbers.

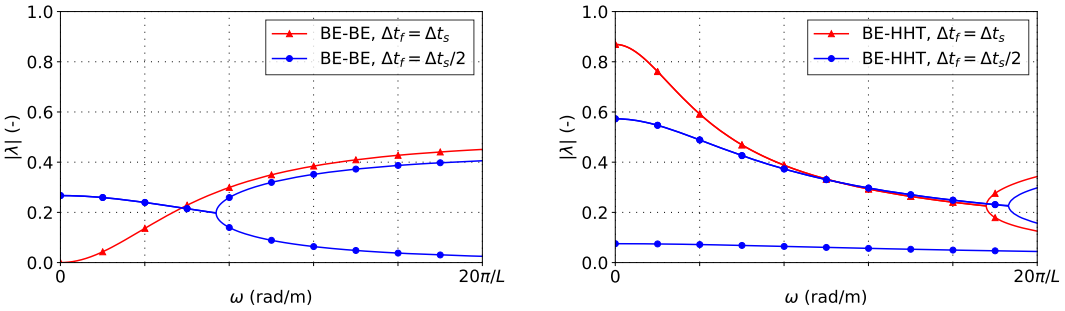

(a) BE-BE (b) BE-HHT

Figure 2: Effect of subcycling in the flow problem on the amplitude of the eigenvalues corresponding to the spurious modes.

3.2 Numerical partitioned FSI simulation

The stability of the FSI simulation is investigated for two values of $N_{S/F}$: $N_{S/F} = 2$ and $N_{S/F} = 10$. The coupling iterations are drawn schematically for $N_{S/F} = 2$ in Figure 3: each coupling iteration contains one time step in the structural solver and two subcycles in the flow solver. A stable solution is obtained for both combinations of time integration schemes for a flow time step size $\Delta t_f = \Delta t_s/2$ and a cubic wall displacement throughout

the subcycles. This is in agreement with the results from the stability analysis shown in Figure 2.

As noted before, the inlet velocity's derivative has a discontinuity at time 0. Consequently, a pressure oscillation occurs after time 0, which should exhibit a decreasing (or at least constant) amplitude as a function of time in case of a temporally stable solution. Therefore, the temporal evolution of the inlet pressure can be used to denote whether the simulation is stable. Figure 4 depicts the inlet pressure evolution throughout the subcycles during the first 15 time steps for a simulation using 2 (red curve) and 10 subcycles (blue curve), respectively. During the first subcycle of each time step a peak in inlet pressure can be observed. The amplitude of this peak decreases in each consecutive time step, confirming that the solution is temporally stable. Meanwhile, this peak continues to exist for the BE-HHT combination, leading to a discrepancy in pressure compared to the solution obtained with matching time steps. According to the foregoing analysis, the subcycling procedure should yield a temporally stable solution even for the BE-HHT scheme. This is in fact confirmed by the numerical simulation as the pressure oscillation does not grow over time. However, it is clear that the BE-BE scheme yields a more accurate result than the BE-HHT scheme as no pressure peaks are triggered at the beginning of each time step. It can be concluded that applying the same discretization scheme in flow and structural solver is beneficial with respect to the removal of oscillations in the solution. This could not be concluded from the analytical study presented in Section 3.1.

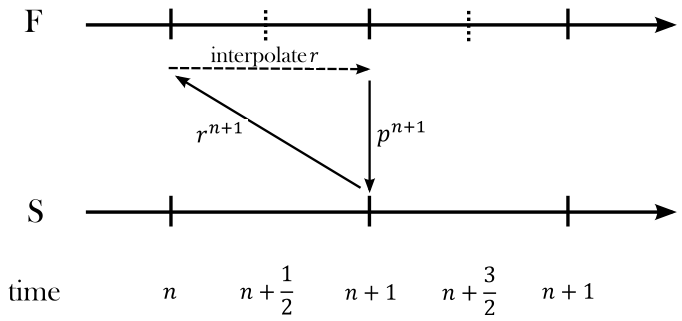

Figure 3: Schematic representation of the coupling iterations in the strongly-coupled FSI problem, in case $N_{S/F} = 2$. The displacement and the pressure of the fluid-structure interface are represented by r and p, respectively. The superscript denotes the time step. The transient structure (S) and flow (F) problem are depicted as separate timelines, whereas the full lines indicate the communication between the solvers. The dotted lines show other operations not related to communication between the solvers. The 'interpolate' procedure denotes the distribution of the interface displacement over the subcycles.

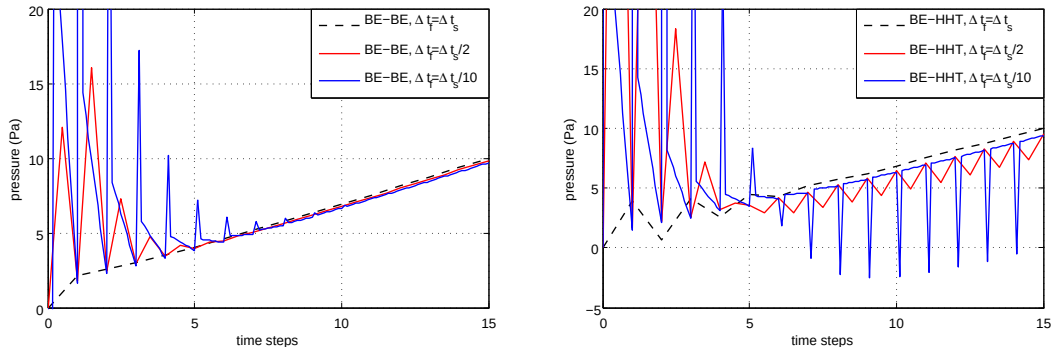

(a) (b)

Figure 4: Effect of subcycling in the flow problem on the evolution of the inlet pressure using (a) the BE-BE combination and (b) the BE-HHT combination.

4 CONCLUSION

The temporal stability of a subcycling procedure in the flow solver is investigated both analytically and numerically. The analytical study of a monolithic FSI calculation is used to quantify the eigenvalues of the matrix relating the flow variables in subsequent time steps. From this, it is concluded that subcycling in the flow solver is temporally stable for all values of $N_{S/F}$, for both the BE-BE and BE-HHT discretization. This conclusion was confirmed with the partitioned numerical FSI simulation, up to $N_{S/F} = 10$. It was furthermore shown that unwanted oscillations can persist in calculations where different temporal discretization schemes are applied to the flow and structural equations, despite the solution being temporally stable.

5 ACKNOWLEDGMENTS

The authors gratefully acknowledge the funding by the Research Foundation-Flanders (FWO), through the Ph.D. fellowship of Laurent De Moerloose. This research was also funded directly by FWO (project nr 3G008509).

REFERENCES

[1] De Ridder, J., Degroote, J., Van Tichelen, K., Schuurmans, P. and Vierendeels, J. Predicting turbulence-induced vibration in axial annular flow by means of large-eddy simulations. *J. Fluids Struct.* (2016) **61**:115–131.

[2] Farhat, C., Lesoinne, M. and Stern, P. High performance solution of three-dimensional nonlinear acoustic problems via parallel partitioned algorithms: methodology and preliminary results. *Adv. Eng. Software* (1997) **28**:43–61.

[3] Piperno, S., Farhat, C. and Larrouturou, B. Partitioned procedures for the transient solution of coupled aeroelastic problems. *Comput. Methods Appl. Mech. Eng.* (1995) **124**:79–112.

[4] Zhang, Q. and Cen, S. Multiphysics modeling: Numerical methods and engineering methods. *Tshingua University Press Limited* and *Elsevier Inc.* (2016).

[5] Causin, P., Gerbeau, J. and Nobile, F. Added-mass effect in the design of partitioned algorithms for fluid-structure problems. *Comput. Methods Appl. Mech. Eng.* (2005) **194**:4506–4527.

[6] De Moerloose, L., Taelman, L., Segers, P., Vierendeels, J. and Degroote, J. Analysis of several subcycling schemes in partitioned simulations of a strongly coupled fluid-structure interaction. *Int. J. Numer. Methods Fluids* (2018) **89**:181–195.

[7] Perktold, K. and Rappitsch, G. Mathematical modelling of local arterial flow and vessel mechanics. *Computation Methods for Fluid Structure Interaction. Pitman Research Notes in Mathematics* (1994):203–245.

[8] Degroote, J., Annerel, S. and Vierendeels, J. Stability analysis of Gauss-Seidel iterations in a partitioned simulation of fluid-structure interaction. *Comput. Struct.* (2010) **88**:263–271.

[9] Hilber, H., Hughes, T. and Taylor, R. Improved numerical dissipation for time integration algorithms in structural dynamics. *Earthq. Eng. Struct. Dyn.* (1977) **5**: 283–292.

[10] Newmark, N. A method of computation for structural dynamics. *ASCE Journal of the Engineering Mechanics Division* (1959) **5**:67–94.

[11] Degroote, J., Bathe, K. and Vierendeels, J. Performance of a new partitioned procedure versus a monolithic procedure in fluid-structure interaction. *Comput. Struct.* (2009) **87**:793–801.